RPS4XL encoded by lnc-Rps4l inhibits hypoxia-induced pyroptosis by binding HSC70 glycosylation site

Yiying Li,[1,6] Junting Zhang,[1,6] Hanliang Sun,[1] Xiufeng Yu,[2] Yujie Chen,[1] Cui Ma,[2] Xiaodong Zheng,[3] Lixin Zhang,[4] Xijuan Zhao,[2] Yuan Jiang,[1] Wei Xin,[1] Shanshan Wang,[1] Jiye Hu,[4] Mingge Wang,[5] and Daling Zhu[1,2]

[1]Biopharmaceutical Key Laboratory of Heilongjiang Province, College of Pharmacy, Harbin Medical University, Harbin 150081, Heilongjiang Province, P.R. China; [2]Central Laboratory of Harbin Medical University (Daqing), Xinyang Road, Gaoxin District, Daqing 163319, P.R. China; [3]Department of Genetic And Cell Biology, Harbin Medical University (Daqing), Daqing 163319, P. R. China; [4]College of Medical Laboratory Science and Technology, Harbin Medical University, Daqing, Heilongjiang Province, China; [5]Harbin Medical University, Harbin 150081, Heilongjiang Province, P.R. China

Pyroptosis is involved in pulmonary hypertension (PH); however, whether this process is regulated by long non-coding RNAs (lncRNAs) is unclear. Some lncRNAs encode peptides; therefore, whether the regulation of pyroptosis in PH depends on lncRNAs themselves or their encoded peptides needs to be explored. We aimed to characterize the role of the peptide RPS4XL encoded by lnc-Rps4l and its regulatory mechanisms during pyroptosis in PH. Transgenic mice overexpression of lnc-Rps4l was established to rescue the inhibition of hypoxia-induced pyroptosis in pulmonary artery smooth muscle cells (PASMCs). An adeno-associated virus 9 construct with a mutation in the open reading frame of lnc-Rps4l was used to verify that it could inhibit hypoxia-induced PASMCs pyroptosis through its encoded peptide RPS4XL. Glutathione S-transferase (GST) pull-down assays revealed that RPS4XL bound to HSC70, and microscale thermophoresis (MST) was performed to determine the HSC70 domain that interacted with RPS4XL. Through glycosylation site mutation, we confirmed that RPS4XL inhibited hypoxia-induced PASMCs pyroptosis by regulating HSC70 glycosylation. Our results showed that RPS4XL inhibits pyroptosis in a PH mouse model and hypoxic PASMCs by regulating HSC70 glycosylation. These results further clarify the important mechanism of vascular remodeling in PH pathology.

INTRODUCTION

The rise in pulmonary arterial pressure and pulmonary vascular resistance during pulmonary hypertension (PH) can lead to right heart failure.[1,2] PH is the third most serious cardiovascular disease, making it a significant public health risk. The pathological changes in this process are extremely complicated and, among them, pulmonary vascular remodeling (PVR) mainly manifests as dysfunction of the pulmonary vascular endothelium, pulmonary artery smooth muscle cell (PASMC) accumulation, and adventitial fibroblasts.[3,4] Additionally, the formation of PVR can also include pathological processes such as proliferation, apoptosis, autophagy, and ferroptosis.[5–9] The

discovery of new pathological changes is undoubtedly a key to revealing the complex pathological process of PVR.

Pyroptosis is a novel form of programmed death that manifests as the continuous expansion of the cell membrane until it ruptures and releases inflammatory factors. Pyroptosis is mediated by the inflammasome, which depends on the activation of caspase-1.[10–13] Recently, pyroptosis was reported to occur in hypoxia-induced PVR, leading to PH.[14,15] The hypoxia-induced increase in the GLI1 triggered an increase in the transcription level of *ASC* expression and induced PASMC pyroptosis.[14] Plasma membrane damage causes NLRP3-dependent interleukin (IL)-1β release and induces pyroptosis during *Mycobacterium tuberculosis* infection.[15] Sphingomyelin synthase 1 mediates hepatocyte pyroptosis through the PKC6/NLRC4/caspase-1 axis to trigger non-alcoholic steatohepatitis.[16] Thus, the mechanism of pyroptosis regulation is complicated and the underlying mechanisms require further exploration.

Long non-coding RNAs (lncRNAs) include transcripts that are greater than 200 nt and participate in complicated mechanisms that regulate gene expression, including regulation of transcription, translation, protein modification, and the formation of RNA-protein complexes;[17–20] therefore, lncRNAs could play critical roles in various biological functions and disease processes. Accumulating evidence indicates that lncRNAs are powerful regulators of pyroptosis. For example, the lncRNA H19 initiates microglial pyroptosis and neuronal death in retinal ischemia/reperfusion injury,[21] and knockdown of lncRNAs of maternally expressed 3 binds to miR-18a and alleviates hyperoxia-induced lung injury by inhibiting thioredoxin-interacting protein-mediated pyroptosis. However, the role of
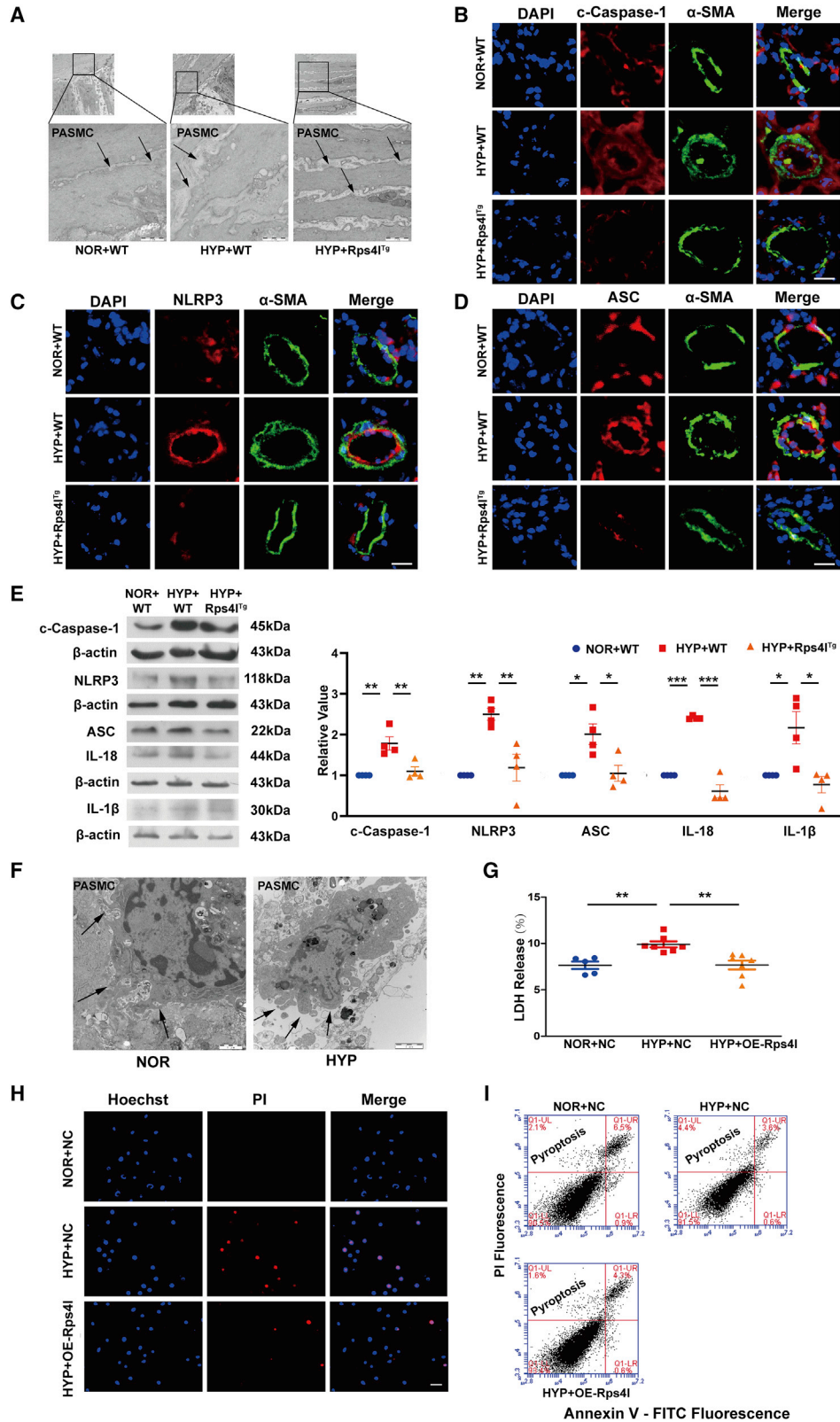
lncRNAs in regulating pyroptosis has not been reported in PH, and, thus, its underlying mechanisms need to be addressed.

Recent studies have shown that some lncRNAs contain short open reading frames (sORFs) that encode functional peptides, and many peptides encoded by lncRNAs are important for disease progression. For example, the peptide CIP2A-BP encoded by LINC00665 inhibits triple-negative breast cancer progression by binding to the CIP2A.[22] Additionally, HOXB-AS3 suppresses colon cancer growth and showed that colon cancer patients with low levels of the HOXB-AS3 peptide had poorer prognoses.[23] A key question that remains is whether the effects of lncRNAs in disease processes are lncRNA dependent or lncRNA-encoded peptide dependent. Our previous study reported that lnc-Rps4l encodes the peptide RPS4XL. RPS4XL is downregulated in hypoxic PASMCs and participates in PH, suggesting that RPS4XL may play a key regulatory role in PH.[24] However, whether RPS4XL is involved in the regulation of PASMC pyroptosis under hypoxia remains unclear.

Our main innovation in this study is to clarify the regulatory mechanism of the peptide RPS4XL encoded by lnc-Rps4l during hypoxic PASMC pyroptosis and the functional domain of RPS4XL. The discovery of the function and mechanism of RPS4XL in pyroptosis regulation will provide a new regulatory network for PVR and help address the complexity of the pathological process of PH to provide more comprehensive therapeutic approaches and targets for PH.

RESULTS

Overexpressed lnc-Rps4l blocks hypoxia-induced pyroptosis in PASMCs *in vivo* and *in vitro*

In order to detect the effect of lncRNA on hypoxia-induced PASMC pyroptosis, we constructed an overexpression transgenic mouse model based on the Rps4l sequence, which was confirmed to be downregulated in hypoxic PASMCs.[25] The tissue specificity and efficiency of lnc-Rps4l overexpression were shown in previous studies.[24,25] After 21 days of hypoxia, the ratio of the right ventricle to the left ventricle plus the ventricular septum was measured, which indicated that lnc-Rps4l overexpression *in vivo* significantly improved right ventricular hypertrophy symptoms caused by hypoxia (Figure S1A). Additionally, ultrasound testing showed that lnc-Rps4l overexpression significantly improved cardiac function in hypoxic mice (Figure S1B) and reversed the hypoxia-induced increase in pulmonary artery pressure (Figure S1C) compared with wild type. In order to more intuitively observe the effect of lnc-Rps4l on pyroptosis in PASMCs, we removed and fixed the lung tissue to observe changes in

cell morphology using electron microscopy. Under hypoxia or normoxia, in the lung tissues of wild-type or lnc-Rps4l-overexpressing mice, we observed PASMCs that were undergoing pyroptosis (Figure 1A). Pyroptosis was detected by immunofluorescence and the results showed that lnc-Rps4l overexpression had a significant inhibitory effect on the expression of the pyroptosis activator caspase-1 that is induced by hypoxia (Figure 1B). In addition, lnc-Rps4l overexpression inhibited the expression of the inflammasome proteins NLRP3 and ASC (Figures 1C and 1D). The same results were obtained by western blotting (Figure 1E). The expressions of inflammatory factors IL-18 and IL-1β were also decreased after overexpression of lnc-Rps4l (Figure 1E). Thus, lnc-Rps4l overexpression improved hypoxia-induced PH *in vivo*.

To further examine the regulatory effect of lnc-Rps4l on pyroptosis *in vitro*, we first detected pyroptosis in PASMCs cultured under normoxic and hypoxic conditions. The results showed that pyroptosis could be detected under these conditions (Figure 1F). Using a lactate dehydrogenase (LDH) release assay and propidium iodide (PI) staining, we showed that the pyroptotic cell death induced by hypoxia was reversed by lnc-Rps4l overexpression (Figures 1G and 1H). The overexpression efficiency of lnc-Rps4l is shown in Figure S2A. Immunoblotting also showed that lnc-Rps4l overexpression inhibited the increased expression of pyroptosis-related indicators that are normally induced by hypoxia (Figures S2B–S2F). Cell flow cytometry experiments also showed that Rps4l reduced hypoxia-induced PASMC pyroptosis (Figure 1I).

lnc-Rps4l contributes to pyroptosis by encoding RPS4XL

After clarifying the regulatory role of lnc-Rps4l in pyroptosis, we further explored its functional mechanism. There are many known mechanisms for lncRNA function, including miRNA adsorption and protein binding.[26,27] However, with the discovery that lnc-Rps4l encodes the functional peptide RPS4XL,[24] we investigated whether lnc-Rps4l can regulate hypoxia-induced PASMCs pyroptosis through encoding peptide RPS4XL, thereby improving vascular remodeling. To test whether RPS4XL regulates pyroptosis, we mutated the open reading frame (ORF) of Rps4l to disrupt the encoding process.[24] We found that the mutation in lnc-Rps4l successfully reversed the increased expression of RPS4XL caused by lnc-Rps4l overexpression (Figure 2A). An LDH release assay and PI staining showed that lnc-Rps4l overexpression inhibited hypoxia-induced pyroptosis in PASMCs, and that this phenomenon could be reversed by expressing the mutant lnc-Rps4l variant (Figures 2B and 2C). Immunoblotting and cell flow cytometry results were consistent with these results,

Figure 1. Overexpression of Rps4l *in vivo* and *in vitro* inhibits hypoxia-induced pyroptosis

(A) Electron micrographs of PASMCs of lung tissues in Rps4lTg and wild-type (WT) hypoxic and normoxic mice. The arrow points to the location of the cell membrane swelling and breakage (down, scale bar, 1 μm). Immunofluorescence analysis of (B) c-caspase-1, (C) NLRP3, (D) ASC in the lung tissues of Rps4lTg and WT hypoxic and normoxic mice (scale bar, 25 μm). Western blotting analysis of (E) c-caspase-1, NLRP3, ASC, IL-1β, and IL-18 in the lung tissues of Rps4lTg and WT hypoxic and normoxic mice. (F) Electron micrographs of hypoxic and normoxic PASMCs. The arrow points to the location of the cell membrane swelling and breakage (right, scale bar, 1 μm; left, scale bar, 2 μm). (G) LDH release assay in hypoxic and normoxic PASMCs transfected with OE-Rps4l or OE-NC. (H) PI staining in hypoxic and normoxic PASMCs transfected with OE-Rps4l or OE-NC (scale bar, 50 μm). (I) Flow cytometry analysis of hypoxic and normoxic PASMCs transfected with OE-Rps4l or OE-NC. All values are represented as the mean ± SEM (*p < 0.05, **p < 0.01, and ***p < 0.001; n ≥ 3). NOR, normoxia; HYP, hypoxia.
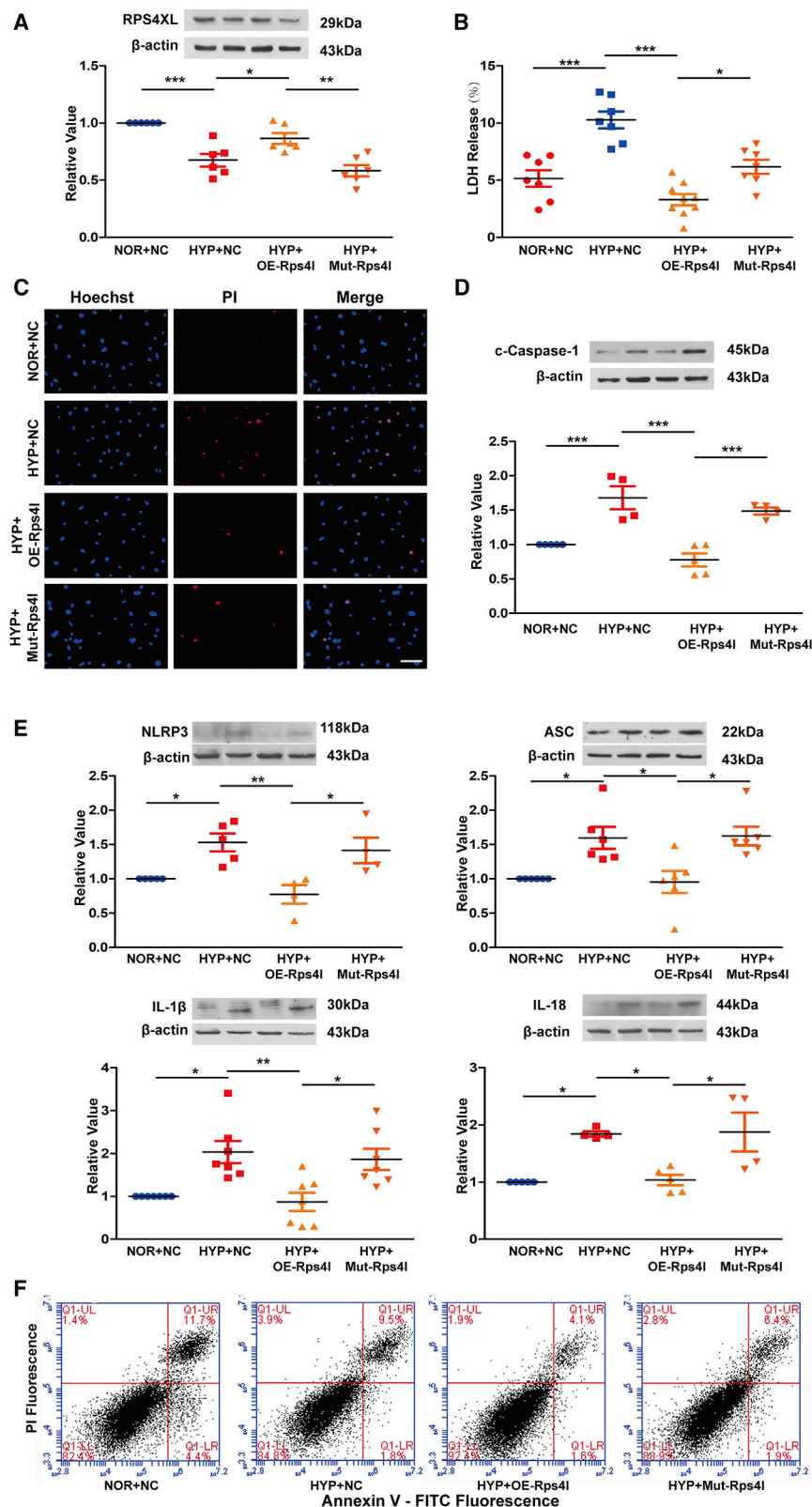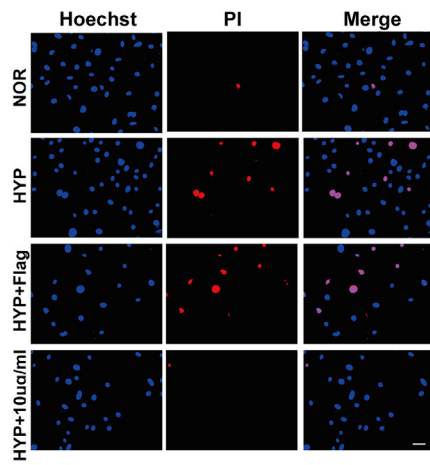
Figure 2. lnc-Rps4l-encoded peptide RPS4XL inhibits hypoxia-induced pyroptosis of PASMCs

(A) Western blotting analysis of RPS4XL in hypoxic and control PASMCs transfected with OE-Rps4l, Mut-Rps4l, or OE-NC. (B) LDH release assay using hypoxic and control PASMCs transfected with OE-Rps4l, Mut-Rps4l, or OE-NC. (C) PI staining in hypoxic and control PASMCs transfected with OE-Rps4l, Mut-Rps4l, or OE-NC (scale bar, 50 μm). Western blotting analysis of (D) c-caspase-1, (E) NLRP3, ASC, IL-1β, and IL-18 in hypoxic and normoxic PASMCs transfected with OE-Rps4l, Mut-Rps4l, or OE-NC. (F) Flow cytometry analysis in hypoxic and control PASMCs transfected with OE-Rps4l, Mut-Rps4l, or OE-NC. All values are represented as the mean ± SEM (*$p < 0.05$, **$p < 0.01$, and ***$p < 0.001$; n ≥ 3). NOR, normoxia; HYP, hypoxia.

A

```
Rps4l Protein Length=268 MW=30001.6 PI=10.97
  1 MARGPKKHLK RVAAPRHWML DKLTGVFAPR PSAGPHRLRE CLPLAIFLRN RLKYALTGDE
 61 VKKICMQRLI KVDGKVRTDV AYPAGFMDVI SIDKSGENFR LVYDTKGRFA VHRITPEEAK
121 YKLCKVRKVF VGTKGIPHLV THDARTIRYP DPLIKVNDTV QISLDSGKIT DAIKFDTGNL
181 CMVTGGANLG RIGVITNRER HPGSFDVVHV KDANGNGFAT RLSNIFVIGK GNKPWISLPR
241 GKGIRLTIAE ERDKRLAAKQ SGHHHHHH
```
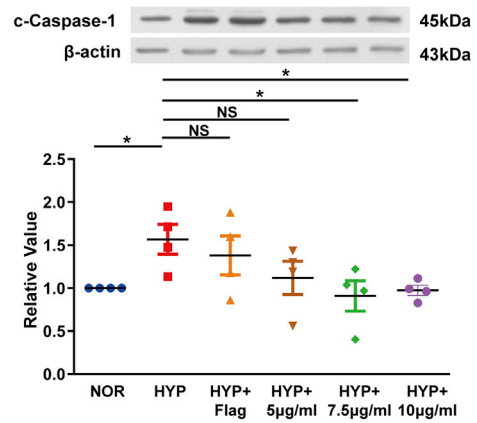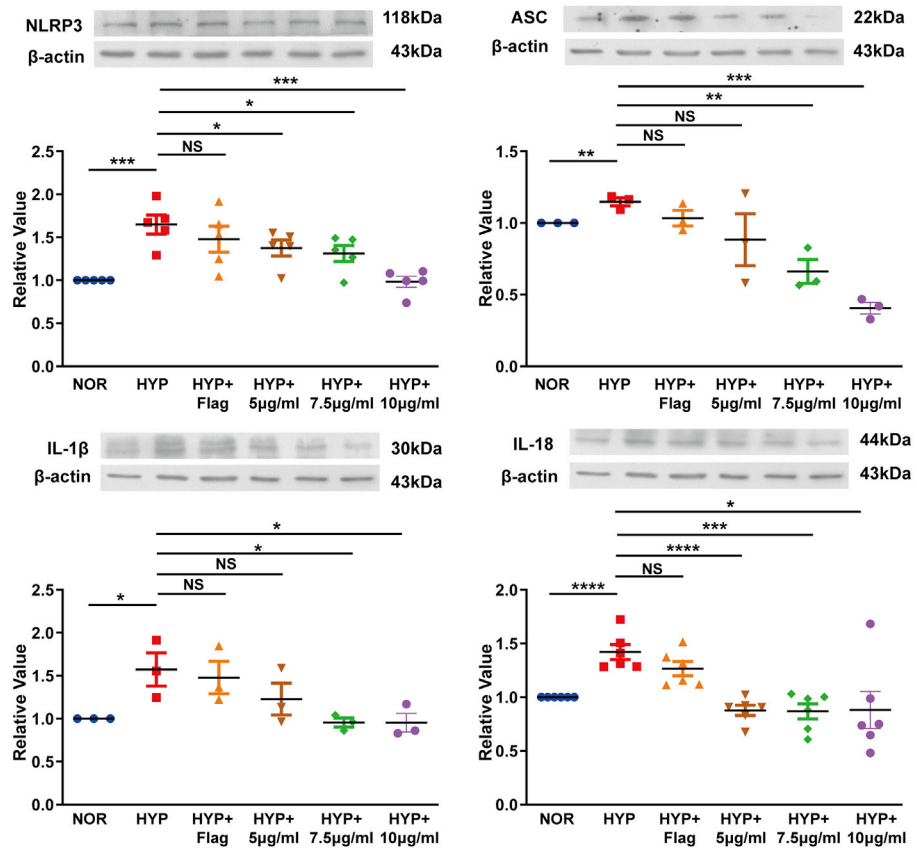
B

C
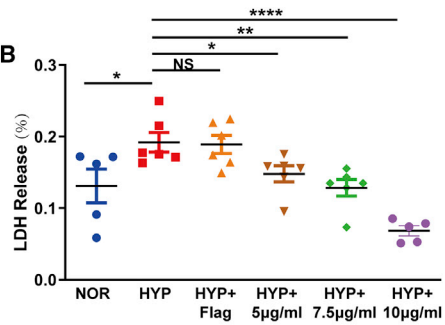
D

E

(legend on next page)

further indicating that lnc-Rps4l inhibits hypoxia-induced PASMC pyroptosis through its encoded peptide RPS4XL (Figures 2D–2F).

This mutant was introduced into the mouse model to test whether RPS4XL functions *in vivo*.[24] After 21 days of hypoxia, the lung tissue proteins in the infected mice by adeno-associated virus 9 were extracted for immunoblotting. We found that the expression of caspase-1, NLRP3, ASC, IL-1β, and IL-18 was upregulated in samples from mice expressing the lnc-Rps4l mutant compared with lnc-Rps4l overexpression lines (Figures S3A–S3E). These results indicate that Rps4l can inhibit hypoxia-induced pyroptosis *in vivo* by encoding the peptide RPS4XL.

The exogenous peptide RPS4XL inhibits hypoxia-induced pyroptosis in PASMCs

To more intuitively explore the regulation of RPS4XL, we purified RPS4XL *in vitro* using its amino acid sequence (Figure 3A). We found that the addition of exogenous RPS4XL effectively inhibited hypoxia-induced PASMC pyroptosis in mice (Figures 3B and 3C), potentially through the inhibition of pyrolysis-related proteins that are induced by hypoxia (Figures 3D and 3E). These results confirmed the regulatory effect of RPS4XL on pyroptosis.

To better explore the function of RPS4XL, we added exogenous RPS4XL to human PASMCs and observed its effect on pyroptosis. Western blotting detected the expression of caspase-1, NLRP3, ASC, IL-1β, and IL-18, indicating that exogenous RPS4XL could inhibit hypoxia-induced pyroptosis in human PASMC (Figures S4A–S4E).

RPS4XL binds to and inhibits the expression of HSC70

To further investigate the downstream regulatory factors of RPS4XL, we constructed an RPS4XL-glutathione S-transferase (GST) fusion protein in an overexpression vector. The GST pull-down assay detected a variety of proteins that directly bind to RPS4XL, which were analyzed then by Gene Ontology (GO) and Kyoto Encyclopedia of Genes and Genomes (KEGG) (Figure 4A). We also predicted proteins that could interact with RPS4XL using bioinformatics (Figure 4B). Among these proteins, HSC70 had the highest mass spectrometry scores of the candidate proteins (Figure 4C). Furthermore, HSC70 was of interest because it was reported to protect against lipopolysaccharide (LPS)-induced inflammatory cell necrosis.[28,29] Therefore, we asked if HSC70 participated in hypoxia-induced pyroptosis. Before selecting HSC70 as the downstream molecule of RPS4XL, we verified that HSC70 could bind to RPS4XL (Figure 4D). Immunoblotting analysis indicated that HSC70 expression was upregulated in hypoxic PASMCs (Figure S5A). In lnc-Rps4l overexpression transgenic hypoxic mouse lung tissue protein, we found that the hypox-

ia-induced upregulation of HSC70 was inhibited (Figure S5B). These *in vivo* and *in vitro* experiments showed that overexpression of lnc-Rps4l inhibits the expression of HSC70 induced by hypoxia, but this phenomenon is reversed by the mutant ORF (Figures 4E and 4F). In addition, the addition of exogenous RPS4XL also downregulated HSC70 expression in hypoxic PASMCs (Figure S5C). Based on the above results, we believe that the regulatory effect of lnc-Rps4l on HSC70 occurred through its encoded peptide RPS4XL.

Interference of HSC70 inhibits hypoxia-induced pyroptosis in PASMCs

To understand the relationship between HSC70 and pyroptosis, we constructed an HSC70 interference model (Figures S6A and S6B). Using an LDH release assay and PI staining, we found that interfering with HSC70 inhibited PASMC pyroptosis caused by hypoxia (Figures S7A and S7B). Western blotting showed that HSC70 interference inhibited the upregulation of hypoxia-induced pyroptosis-related indicators (Figures S7C–S7G), indicating that HSC70 can participate in the regulation of hypoxia-induced PASMC pyroptosis.

### The domain of RPS4XL regulates cell pyroptosis and HSC70

We have previously described the regulatory role of Rps4l on pyroptosis and HSC70, but we did not clarify its functional domain of RPS4XL. To do this now, due to the structural similarity with RPS4X, RPS4XL is divided into three segments according to the RPS4X domains on Uniprot. We created the overexpression constructs of each domain: 1–41 amino acids (aa), 42–104 aa, and 105–262 aa. The spatial structure of the three RPS4XL domains are shown in Figure 5A. The global and local quality estimates and standardized QMEAN4 scores for the structural model are shown in Figure S8. After transfecting the overexpression domain constructs into mouse PASMCs, we found that overexpression of the second and third RPS4XL domains inhibited the increased expression of HSC70 that is induced by hypoxia (Figure 5B). Subsequent PI staining and LDH release assays showed that the second domain of RPS4XL was involved in the regulation of pyroptosis (Figures 5C and 5D). Therefore, the second domain of RPS4XL participates in the inhibition of hypoxia-induced pyroptosis-related indicators (Figures 5E and 5F), potentially through its inhibitory effect on hypoxia-induced HSC70 expression.

RPS4XL inhibits hypoxia-induced pyroptosis in PASMCs by inhibiting HSC70 glycosylation

After clarifying the specific domains that support RPS4XL function, we wanted to further explore the regulatory mechanism of HSC70. We divided HSC70 into three segments according to its domains for *in vitro* purification and fluorescein isothiocyanate (FITC) labeling. After mixing the three labeled fluorescent protein fragments

Figure 3. Exogenous RPS4XL treatment of PASMCs inhibits hypoxia-induced pyroptosis

(A) Synthetic sequence of the exogenous peptide RPS4XL. (B) LDH release assay using PASMCs treated with 5 μg/mL, 7.5 μg/mL, or 10 μg/mL exogenous RPS4XL under hypoxia. (C) PI staining in PASMCs treated with 10 μg/mL RPS4XL under hypoxia (scale bar, 50 μm). Western blotting analysis of (D) c-caspase-1, (E) NLRP3, ASC, IL-1β, and IL-18 in PASMCs treated with 5 μg/mL, 7.5 μg/mL, or 10 μg/mL RPS4XL under hypoxia. FLAG was used as a negative control. All values are represented as the mean ± SEM (*p < 0.05, **p < 0.01, and ***p < 0.0001; n ≥ 3). NOR, normoxia; HYP, hypoxia.

A

B

C

Gene name Hspa8, Hspa2
Score 341.79
m/z 740.88

A R F E E L N A D L F R

D

E

F
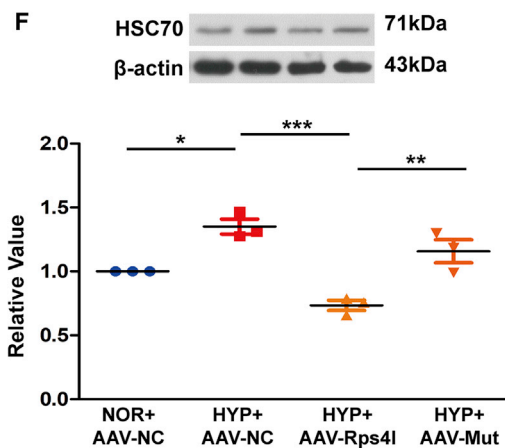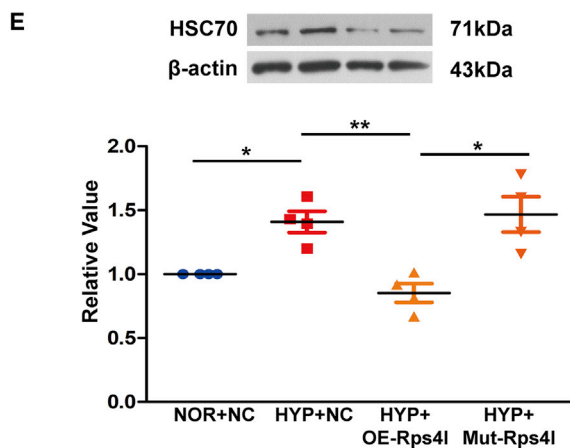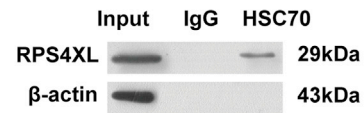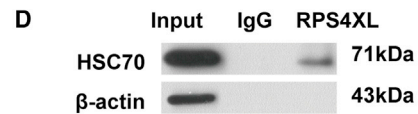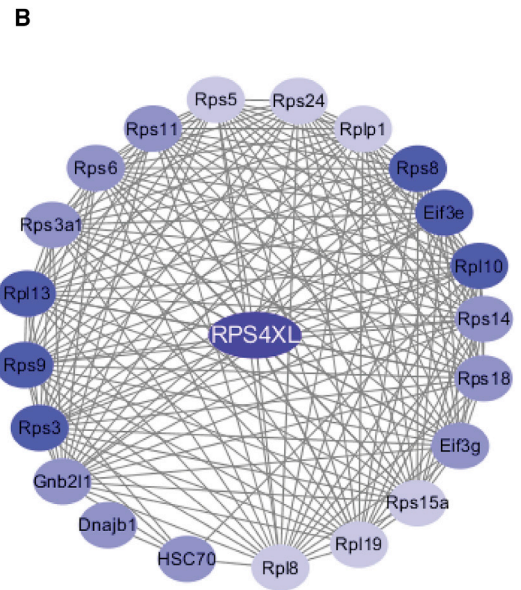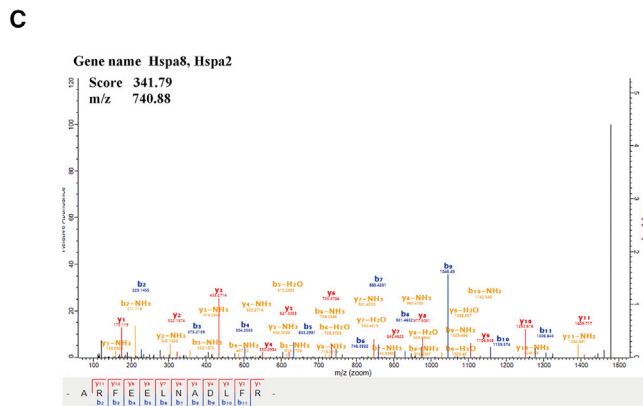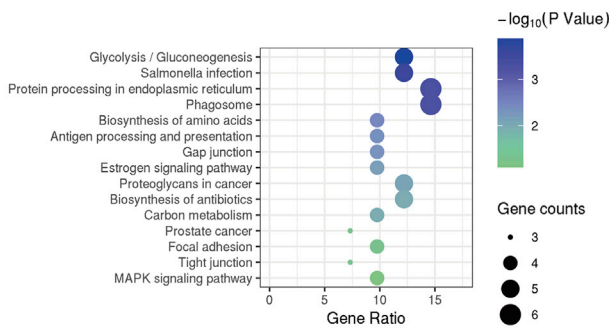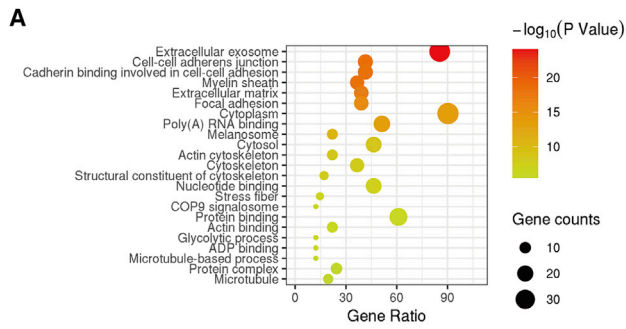
(legend on next page)

with exogenous RPS4XL, microscale thermophoresis showed that the first domain of HSC70 (1–393 aa) has a strong intermolecular interaction with RPS4XL (Figure 6A), while the other two domains did not (Figures S9A and S9B). Protein glycosylation is one of the most common post-translational modifications of proteins and can change the conformation of polypeptides and increase protein stability.[30–32] Therefore, we predicted that the first segment domain of HSC70 contained glycosylation sites glycosylation. Using bioinformatics, we found that there were only four N-glycosylation sites in the first domain of HSC70 (Figures 6B, S10A, and S10B) and no O-glycosylation sites (Figures S10C and S10D). Next, the glycosylation inhibitor tunicamycin was used to verify the effect of glycosylation on hypoxic PASMC pyrolysis. We found that the addition of tunicamycin effectively inhibited the expression of HSC70 and pyroptosis induced by hypoxia (Figures S11A–S11G). To determine whether RPS4XL regulates pyrolysis by affecting HSC70 glycosylation, we mutated the predicted N-glycosylation site in the HSC70 first domain (Figure 6B). We found that the addition of exogenous RPS4XL inhibited hypoxia-induced PASMC pyroptosis, and could be reversed by overexpression of HSC70. However, when the N-glycosylation site of HSC70 was mutated, HCS70 could not inhibit the effects of RPS4XL (Figures 6C–6F). Therefore, RPS4XL inhibits hypoxia-induced PASMC pyroptosis by binding to HSC70 and inhibiting its glycosylation.

DISCUSSION

In this study, the new discovery is that we found the peptide RPS4XL encoded by lnc-Rps4l relieved PH by inhibiting pyroptosis in PASMCs. The mechanism by which RPS4XL functions is through its binding to HSC70 and inhibition of HSC70 glycosylation. These results suggest that RPS4XL plays an important regulatory role in hypoxia-induced PVR, which is a critical event in the PH.

LncRNA was considered to be an RNA molecule with no coding ability that participated in different disease, such as cardiovascular diseases, malignant tumors, respiratory diseases, and PH.[33–35] It has been reported that the lncRNA TYKRIL acts as a protein decoy that contributes to PH via the p53-mediated regulation of PDGFRβ.[36] Moreover, the lncRNA TUG1 regulates PASMC proliferation by adsorbing miR-328–3p.[37] Most studies of lncRNAs have focused on their function, but recent studies have shown that some lncRNAs have sORFs that can be translated into functional small peptides.[38–41] For example, a peptide encoded by the lncRNA HOXB-AS3 suppresses colon cancer growth and the SRSP peptide encoded by lncRNA LOC90024 contributes to RNA splicing in colorectal cancer.[23,42] We also found that RPS4XL encoded by the lnc-Rps4l was

involved in hypoxia-induced PASMC proliferation in PH.[24] These findings undoubtedly fill the gap in our understanding of the functions of lncRNA-encoded peptides in PH.

Because the mechanisms that lead to PVR are not limited to PASMC proliferation, other potential functions of RPS4XL in PVR need to be explored. More importantly, whether the role of lncRNAs in PH depends on whether the lncRNAs themselves or their encoded peptides need to be identified. Our current research answers a key scientific question: does the Rps4l-encoded peptide RPS4XL or the lnc-Rps4 regulate the pathological process of pyroptosis?

Pyroptosis is a type of inflammasome-mediated programmed necrosis that participates in the process of hypoxia-induced PVR.[8,14] Hypoxia can induce the expression of caspase-1, which aggravates PASMC pyroptosis and causes pulmonary artery fibrosis.[43,44] However, the mechanism of caspase-1 activation during pyroptosis remains unclear. In this study, we used *in vivo* overexpression transgenic mouse and adeno-associated virus mouse models, *in vitro* overexpression and mutation constructs, and the addition of exogenous RPS4XL to show that lnc-Rps4l can encode the peptide RPS4XL, which inhibits hypoxia-induced caspase-1. Our results showed that lnc-Rps4l had a significant inhibitory effect on the hypoxia-induced expression of pyroptosis activator caspase-1 both *in vivo* and *in vitro*, and the effect was dependent on its encoded peptide RPS4XL, which serves as a trigger that activates pyroptosis.

Our previous study confirmed that RPS4XL has the ability to inhibit hypoxia-induced PASMC proliferation and does not conflict with the inhibition of hypoxia-induced PASMC pyroptosis by RPS4XL demonstrated in this study. Under hypoxic conditions, PASMC proliferation caused vascular wall thickening and increased pyroptosis-induced fibrosis, which led to PVR.[45,46] What causes PVR is a complex molecular regulatory network. We explored RPS4XL inhibition of hypoxia-induced PASMC proliferation by reducing RPS6 phosphorylation, and inhibited hypoxia-induced PASMC pyroptosis by inhibiting HSC70 glycosylation. Our study demonstrates that RPS4XL regulates proliferation and pyroptosis through different signaling pathways, leading to PVR. The discovery that RPS4XL inhibits hypoxia-induced PASMC pyroptosis provides a potential therapeutic target for PH vascular remodeling. This is the first study to confirm the multiple functions of lncRNA-encoded peptides in the regulation of PH, and further reveals the importance of lncRNA-encoded peptide research.

Another important and novel finding of our study was the identification of HSC70 as a key protein that regulates pyroptosis in PASMCs

Figure 4. RPS4XL interacts with HSC70

(A) GO and KEGG analysis of the proteins isolated by a GST pull-down assay using RPS4XL. (B) Bioinformatics prediction of the RPS4XL interaction network. (C) Mass spectrometry of specific segments of HSC70. (D) Western blotting analysis of HSC70 expression in PASMCs transfected with the ORF-FLAG construct under normoxia after co-immunoprecipitation (coIP) using an anti-FLAG antibody (top), and RPS4XL in PASMCs under normoxia after coIP using an anti-HSC70 antibody (bottom). (E) HSC70 protein expression in hypoxic and normoxic PASMCs transfected with OE-Rps4l, Mut-Rps4l, or OE-NC. (F) Western blotting analysis of HSC70 in the lung tissues of hypoxic mice infected with serotype 9 adenovirus-associated virus (AAV9)-NC, AAV9-Rps4l, and AAV9-mut. All values are represented as the mean ± SEM (*p < 0.05, **p < 0.01, and ***p < 0.001; n ≥ 3). NOR, normoxia; HYP, hypoxia.
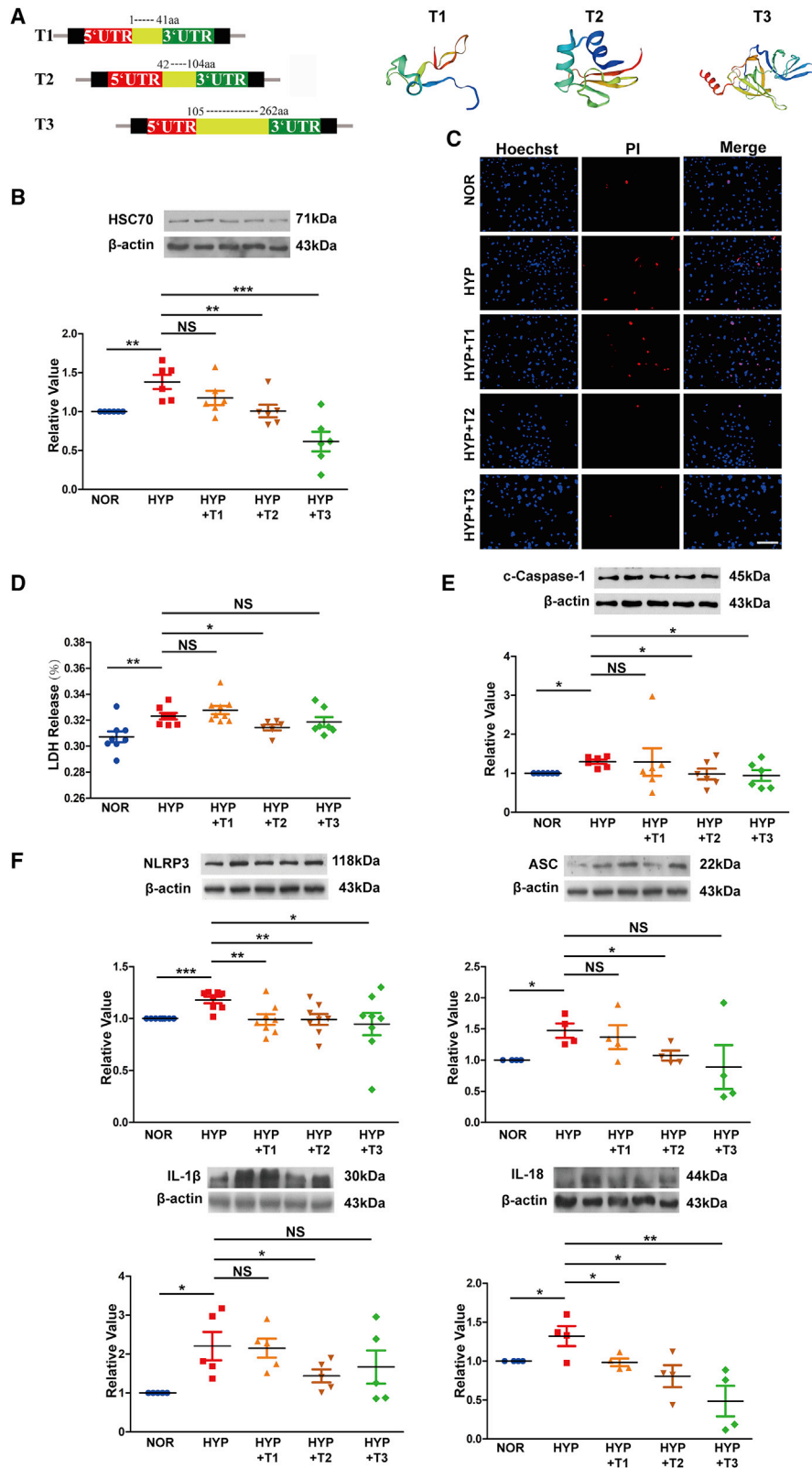
in response to hypoxia. Indeed, *HSC70* knockdown in PASMCs resulted in attenuated hypoxia-induced pyroptosis. HSC70 participates in a variety of metabolic processes in organisms, such as promoting the removal of individual peroxisomes affected by oxidative stress.[47] It is also associated with hepatitis C virus particles and can modulate virus infectivity.[48] HSC70 is involved in the transcriptional stimulation of the DNA-binding protein Hap46/BAG-1M, and can bind bacterial LPS to mediate LPS-induced inflammatory responses.[49] In this study, we confirmed for the first time that HSC70 participates in the activation of caspase-1.

RPS4XL inhibits HSC70 N-glycosylation. Glycosylation mainly occurs in the endoplasmic reticulum and Golgi apparatus and is involved in the regulation of various diseases, such as Alzheimer's disease, cancer, and inflammatory diseases.[50–53] However, there are only a few reports of N-glycosylation in PH, suggesting that our understanding of its function is limited. The use of tunicamycin as a glycosylation inhibitor confirmed the role of glycosylation in PH. Furthermore, the combination of RPS4XL and HSC70 glycosylation sites blocked the N-glycosylation process of HSC70, resulting in decreased HSC70 stability and reduced caspase-1 activation.

In conclusion, our results indicate that RPS4XL encoded by lnc-Rps4l plays a significant and unique role in PH by modulating pyroptosis in PASMCs. We demonstrated for the first time that RPS4XL plays a critical regulatory role in pyroptosis *in vivo* and *in vitro* by inhibiting HSC70 N-glycosylation. This finding suggests that RPS4XL is a potential pharmacological target for the treatment of PH.

MATERIALS AND METHODS

Animals

C57BL/6 male mice weighing 20–30 g were obtained from the Experimental Animal Center of Harbin Medical University, and C57BL/6 transgenic mice overexpression of Rps4l were obtained from Beijing Weitongda Biotech.[25] They were randomly divided into normal groups (inhaled oxygen concentration was 0.21) and hypoxic groups (inhaled oxygen concentration was 0.10). After 21 days of breeding, RV/LV + S and right ventricular systolic blood pressure (RVSP) were detection to prove that the hypoxic PH model was successfully constructed. Pentobarbital sodium was injected intraperitoneally at a concentration of 1% and 40 mg/kg to anesthetize mice.

Construction of serotype 9 adenovirus-associated virus and the hypoxic animal model

As previously described,[24] the adeno-associated virus was synthesized by Genechem (Shanghai, China), and the virus infects mice intrana-

sally. After the mice were anesthetized, the lung tissue proteins were extracted after ultrasound and right ventricular pressure were detected, which were directly used for detection.

RNA extraction

The cells were lysed by TRIzol (Invitrogen, Carlsbad, CA, USA) according to the manufacturer's protocol after washing with PBS three times.

Real-time PCR

The isolated RNA was reverse transcribed into cDNA using a reverse transcription kit (Haigene, China). The primers were as follows, *HSC70*: forward primer, 5′-CTTCAATGSCTCTCAGCGACA-3′, reverse primer, 5′-AATAGCAGCAGCAGTTGGTTC-3′.

siRNA and plasmid design and transfection

Cell density was cultivated to 50%–60%. Specific small interfering RNAs (siRNAs) (Guangzhou, China) and X-treme were used in the transfection process. Corresponding detection was performed 24 h after transfection. si-*HSC70* target sequence: GATGAGAAGCAG AGAGATA. The plasmids were synthesized by Genechem (Shanghai, China) according to the sequence.

Western blot analysis

RIPA lysis buffer (Beyotime, Shanghai, China) was used to extract tissue or cell proteins, and 10%–12% polyacrylamide gels were prepared for protein separation. After the proteins on the gel were transferred to the nitrocellulose membrane, they were incubated with 5% milk for 1 h. Primary antibodies against caspase-1 (1:250), NLRP3 (1:500), ASC (1:400), IL-1β (1:400), IL-18 (1:1,000), HSC70 (1:1,000), and RPS4XL (1:2000) were used, with β-actin (1:3,000) as an internal control. The corresponding primary antibody, secondary antibody, and ECL (Beyotime, Shanghai, China) were incubated for chemiluminescence detection.

Immunofluorescence

The corresponding lung tissue frozen section was prepared and placed at room temperature for 20 min before proceeding to the next step, in which 4% paraformaldehyde was used to soak the sections to fix the tissue. Then PBS was used to wash three times, 5 min each time, and 0.3% Triton X-100 was added for 30 min at 37°C. After washing three times with PBS, it was incubated for 30 min at 37°C with 5% BSA. Subsequently, the tissues were incubated with anti-caspase-1 antibody (1:100), anti-NLRP3 antibody (1:100), or anti-ASC antibody (1:100) mixed with anti-α-SMA antibody (1:100) at 4°C overnight. After washing three times with PBS, fluorescently labeled secondary antibody was used to incubate for 2 h at 37°C. After washing three times with PBS, DAPI was incubated

Figure 5. The functional domain of RPS4XL

(A) Schematic diagram of the vector construction with the different RPS4XL domains. SWISS-MODEL schematic structural model of the different RPS4XL domains. (B) HSC70 protein expression in hypoxic and normoxic PASMCs overexpressing RPS4XL 1–41 aa, 42–104 aa, and 105–262 aa domains. (C) PI staining in hypoxic and normoxic PASMCs overexpressing the RPS4XL 1–41 aa, 42–104 aa, and 105–262 aa domains (scale bar, 100 μm). (D) LDH release assay in hypoxic and normoxic PASMCs overexpressing the RPS4XL 1–41 aa, 42–104 aa, and 105–262 aa domains. Western blotting analysis of (E) c-caspase-1, (F) NLRP3, ASC, IL-1β, and IL-18 in hypoxic and normoxic PASMCs overexpressing the RPS4XL 1–41 aa, 42–104 aa, and 105–262 aa domains. All values are represented as the mean ± SEM (*p < 0.05, **p < 0.01, and ***p < 0.001; n ≥ 3). NOR, normoxia; HYP, hypoxia; NS, no significance.
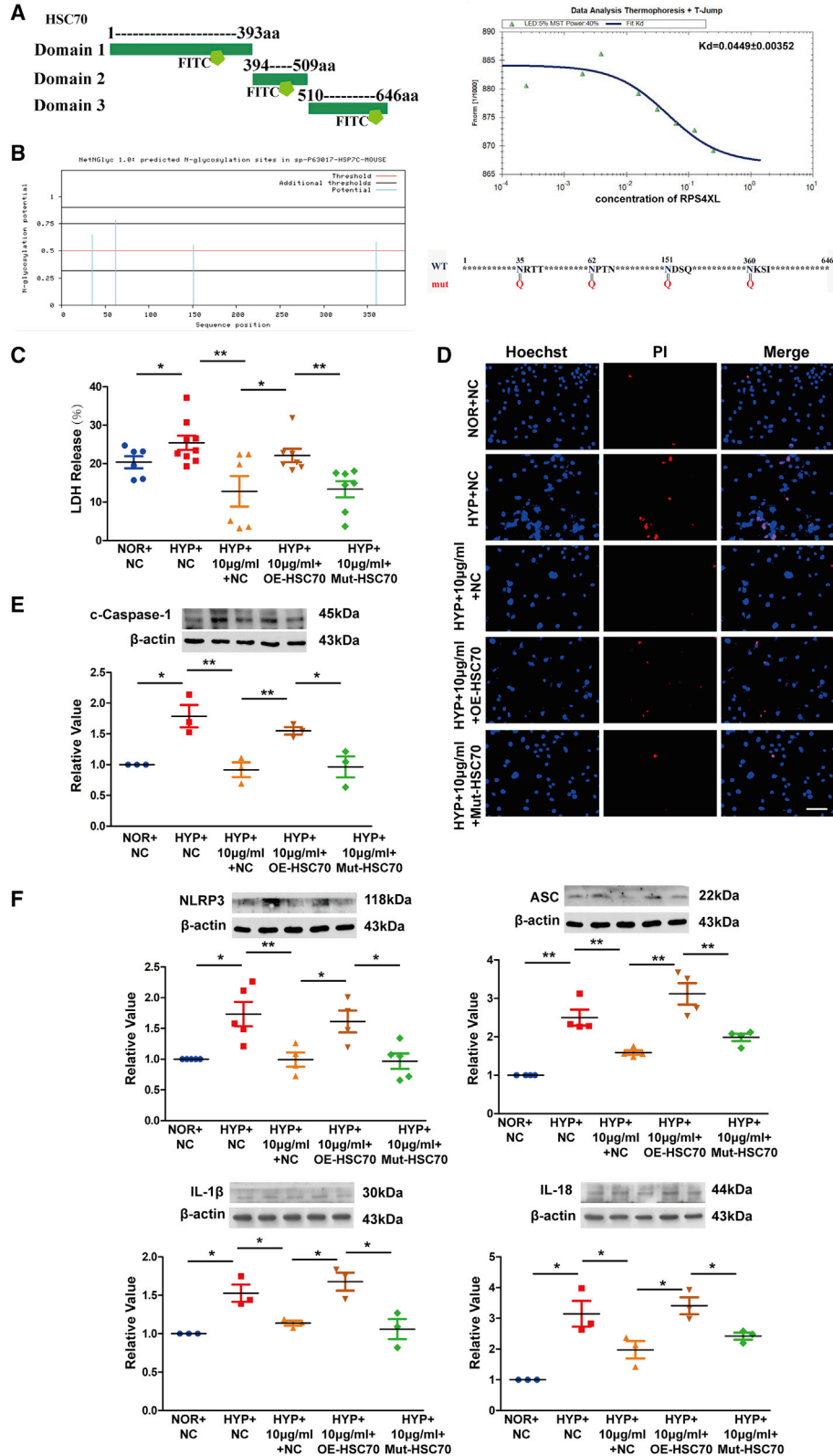
(legend on next page)

at room temperature for 15 min. Confocal laser scanning microscope (CLSM) was used to acquire images.

Electron microscopy

For lung tissue sample preparation, after the animals were anesthetized with sodium pentobarbital, the lung tissues were removed, and the pulmonary arteries were dissected. Then 2.5% glutaraldehyde was dripped for fixation. A new, oil-free sharp (double-sided) blade was used to cut the material into small pieces about 1 mm wide and 1 mm long. Finally, the small piece was placed into the EP tube filled with cold fresh fixative, and put into the refrigerator compartment to fix at low temperature ($0 \sim 4°C$).

For cell sample preparation, PASMCs were cultured in a small cell flask, the culture solution was poured out first, then an appropriate amount of glutaraldehyde fixative was added, it was placed in an ice bath for 3 to 5 min, then the cells gently scraped on the bottle wall with a spatula, the fixative containing the cells was transferred to a centrifuge tube and centrifuged at low speed (2,000 rpm) for 15 min to make the cells aggregate into clumps, and the supernatant was discarded and replaced with fresh fixative to continue fixing.

The prepared samples were submitted to the Harbin Veterinary Research Institute of the Chinese Academy of Agricultural Sciences for further testing.

Cell flow cytometry

As previously described,[54] PASMCs were cultured at 60%–70% density, and the cells were transfected with siRNA or treated with drugs. The cell culture medium was aspirated into a suitable centrifuge tube, and the cells were washed with PBS. An appropriate amount of trypsin was added to digest the cells until the cells could be beaten down. The previously collected cell culture fluid was added to stop the digestion, and it was centrifuged at $1,000 \times g$ for 5 min. The supernatant was discarded, the cells were collected, 195μL of Annexin V-FITC-binding solution was added, and the cells were gently resuspended. Next, 5μL of Annexin V-FITC was added and mixed gently, then 10μL of potassium iodide staining solution was added and mixed gently. It was incubated for 15 min in the dark at room temperature. The cells were resuspended three times during the incubation process for flow cytometry. All reagents used were purchased from Beyotime C1062L (Shanghai, China).

Purification and use of exogenous peptides

As previously described,[24] the exogenous peptide was synthesized by Detaibio (Nanjing China) and added to the cell culture medium at the corresponding concentration.

PI staining

PASMCs were cultured in 24-well plates at 60%–70% density, and the cells were transfected with siRNA or treated with drugs. Next, 8 μL of Hoechst 33342 solution was added, the cells were incubated at 37°C for 10 min, followed by straining with 3 μL of PI for 15 min. The incubation process was carried out in the dark.

GST pull-down and mass spectrometry

Rps4l-GST fusion plasmid was synthesized by Genechem (Shanghai, China), and was transfected into PASMCs. Next, protein lysate was sent to BiotechPack (Beijing, China) for GST pull-down and mass spectrometry.

LDH assay

PASMCs were cultured in 96-well plates at 60%–70% density, the cells were transfected with siRNA or treated with drugs, and 120 μL of $400 \times g$ centrifuged culture solution was pipetted. Next, 60μL of LDH test solution was added at 25°C in the dark for 30 min. The absorbance was then measured at 490 nm.

Co-immunoprecipitation assay

To cultivate PASMCs, after the cells were full, the culture medium was discarded, washed with PBS three times, and then cell lysate was added. After centrifugation at 13,500 rpm at 4°C, the supernatant was collected. Then the corresponding antibody was added overnight at 4°C. Next day, it was incubated with protein A + G magnetic beads for 3 h. After centrifugation, the supernatant was carefully removed, and PBS was added to the pellet, which was repeated five times. The resulting protein was used for further detecting.

Microscale thermophoresis

For microscale thermophoresis (MST) experiments, RPS4XL synthesis was done by Detaibio (Nanjing China). HSC70 was divided into three segments according to its structural domain, which was synthesized by Zoonbio (Nanjing, China) and labeled with FITC. Four microliters of FITC-labeled HSC70 fragment and 6 μL of RPS4XL of different concentration gradients were mixed. A Monolith NT.115 system (NanoTemper Technologies, Munich, Germany) was used for measurements.[55]

Use of glycosylation inhibitors

Tunicamycin (Tu, ab120296) was purchased from Abcam (Cambridge, MA, USA) and dissolved in DMSO. Tu was added to the PASMC culture medium at a concentration of 1 μg/mL.[56] After 24 h, the corresponding assay was performed.

Figure 6. RPS4XL inhibits HSC70 glycosylation, which inhibits hypoxia-induced pyroptosis in PASMCs

(A) Schematic diagram of the *in vitro* purification of the HSC70 protein domains. Microscale thermophoresis of the HSC70 1–393 aa and different concentrations of RPS4XL. (B) Bioinformatics analysis the N-glycosylation site in the 1–393 aa domain of HSC70, and schematic diagram of the HSC70 glycosylation site mutation. (C) LDH release assay in hypoxic and normoxic PASMCs transfected with OE-HSC70, Mut-HSC70, or treated with 10 μg/mL RPS4XL. (D) PI staining in hypoxic and normoxic PASMCs transfected with OE-HSC70, Mut-HSC70, or treated with 10 μg/mL RPS4XL (scale bar, 50 μm). Western blotting analysis of (E) c-caspase-1, (F) NLRP3, ASC, IL-1β, and IL-18 in hypoxic and normoxic PASMCs transfected with OE-HSC70, Mut-HSC70, or treated with 10 μg/mL RPS4XL. All values are represented as the mean ± SEM (*p < 0.05, and **p < 0.01; n ≥ 3). NOR, normoxia; HYP, hypoxia.

Bioinformatics analysis

The protein-protein interaction network was analyzed by STRING (https://string-db.org/) and was then visualized using the Cytoscape program (http://cytoscape.org/). GO and KEGG analysis was made by DAVID (https://david.ncifcrf.gov/). Glycosylation site prediction was through NetNGlyc (http://www.cbs.dtu.dk/services/NetNGlyc/) and DictyOGlyc (http://www.cbs.dtu.dk/services/DictyOGlyc/). The construction of the RPS4XL domain model was through SWISS-MODEL (https://swissmodel.expasy.org/).

Statistical analysis

One-way ANOVA followed by Dunnett's test and Student's t tests were used for comparisons among multiple groups and between two groups, respectively. The data were expressed as mean ± SEM. When $p < 0.05$, it was considered statistically significant.

SUPPLEMENTAL INFORMATION

Supplemental information can be found online at https://doi.org/10.1016/j.omtn.2022.05.033.

AUTHOR CONTRIBUTIONS

Y.L., J.Z., H.S., X.Y., Y.C., C.M., X. Zheng., L.Z., X. Zhao, Y.J., W.X., S.W., J.H., and M.W. conducted the experiments. Y.L., J.Z. and D.Z. designed the experiments. Y.L. and D.Z. wrote the paper.

DECLARATION OF INTERESTS

The authors declare no competing interests.

REFERENCES

1. Zelt, J.G.E., Chaudhary, K.R., Cadete, V.J., Mielniczuk, L.M., and Stewart, D.J. (2019). Medical therapy for heart failure associated with pulmonary hypertension. Circ. Res. *124*, 1551–1567. https://doi.org/10.1161/circresaha.118.313650.

2. Hansen, T., Galougahi, K.K., Celermajer, D., Rasko, N., Tang, O., Bubb, K.J., and Figtree, G. (2016). Oxidative and nitrosative signalling in pulmonary arterial hypertension - implications for development of novel therapies. Pharmacol. Ther. *165*, 50–62. https://doi.org/10.1016/j.pharmthera.2016.05.005.

3. Pak, O., Aldashev, A., Welsh, D., and Peacock, A. (2007). The effects of hypoxia on the cells of the pulmonary vasculature. Eur. Respir. J. *30*, 364–372. https://doi.org/10.1183/09031936.00128706.

4. Humbert, M., Guignabert, C., Bonnet, S., Dorfmüller, P., Klinger, J.R., Nicolls, M.R., Olschewski, A.J., Pullamsetti, S.S., Schermuly, R.T., Stenmark, K.R., and Rabinovitch, M. (2019). Pathology and pathobiology of pulmonary hypertension: state of the art and research perspectives. Eur. Respir. J. *53*, 1801887. https://doi.org/10.1183/13993003.01887-2018.

5. Batool, M., Berghausen, E.M., Zierden, M., Vantler, M., Schermuly, R.T., Baldus, S., Rosenkranz, S., and Ten Freyhaus, H. (2020). The six-transmembrane protein Stamp2 ameliorates pulmonary vascular remodeling and pulmonary hypertension in mice. Basic Res. Cardiol. *115*, 68. https://doi.org/10.1007/s00395-020-00826-8.

6. Vitry, G., Paulin, R., Grobs, Y., Lampron, M.C., Shimauchi, T., Lemay, S.E., Tremblay, E., Habbout, K., Awada, C., Bourgeois, A., et al. (2021). Oxidized DNA precursors cleanup by NUDT1 contributes to vascular remodeling in pulmonary arterial hypertension. Am. J. Respir. Crit. Care Med. *203*, 614–627. https://doi.org/10.1164/rccm.202003-0627OC.

7. Zhou, J.J., Li, H., Li, L., Li, Y., Wang, P.H., Meng, X.M., and He, J.G. (2021). CYLD mediates human pulmonary artery smooth muscle cell dysfunction in congenital heart disease-associated pulmonary arterial hypertension. J. Cell. Physiol. *236*, 6297–6311. https://doi.org/10.1002/jcp.30298.

8. Zhang, M., Xin, W., Yu, Y., Yang, X., Ma, C., Zhang, H., Liu, Y., Zhao, X., Guan, X., Wang, X., and Zhu, D. (2020). Programmed death-ligand 1 triggers PASMCs pyroptosis and pulmonary vascular fibrosis in pulmonary hypertension. J. Mol. Cell. Cardiol. *138*, 23–33. https://doi.org/10.1016/j.yjmcc.2019.10.008.

9. Abdul, Y., Li, W., Ward, R., Abdelsaid, M., Hafez, S., Dong, G., Jamil, S., Wolf, V., Johnson, M.H., Fagan, S.C., and Ergul, A. (2020). Deferoxamine treatment prevents post-stroke vasoregression and neurovascular unit remodeling leading to improved functional outcomes in type 2 male diabetic rats: role of endothelial ferroptosis. Transl. Stroke Res. *12*, 615–630. https://doi.org/10.1007/s12975-020-00844-7.

10. Shi, J., Zhao, Y., Wang, K., Shi, X., Wang, Y., Huang, H., Zhuang, Y., Cai, T., Wang, F., and Shao, F. (2015). Cleavage of GSDMD by inflammatory caspases determines pyroptotic cell death. Nature *526*, 660–665. https://doi.org/10.1038/nature15514.

11. Xu, B., Jiang, M., Chu, Y., Wang, W., Chen, D., Li, X., Zhang, Z., Zhang, D., Fan, D., Nie, Y., et al. (2018). Gasdermin D plays a key role as a pyroptosis executor of non-alcoholic steatohepatitis in humans and mice. J. Hepatol. *68*, 773–782. https://doi.org/10.1016/j.jhep.2017.11.040.

12. Wu, C., Lu, W., Zhang, Y., Zhang, G., Shi, X., Hisada, Y., Grover, S.P., Zhang, X., Li, L., Xiang, B., et al. (2019). Inflammasome activation triggers blood clotting and host death through pyroptosis. Immunity *50*, 1401–1411.e4. https://doi.org/10.1016/j.immuni.2019.04.003.

13. Wang, K., Sun, Q., Zhong, X., Zeng, M., Zeng, H., Shi, X., Li, Z., Wang, Y., Zhao, Q., Shao, F., and Ding, J. (2020). Structural mechanism for GSDMD targeting by auto-processed caspases in pyroptosis. Cell *180*, 941–955.e20. https://doi.org/10.1016/j.cell.2020.02.002.

14. He, S., Ma, C., Zhang, L., Bai, J., Wang, X., Zheng, X., Zhang, J., Xin, W., Li, Y., Jiang, Y., et al. (2020). GLI1-mediated pulmonary artery smooth muscle cell pyroptosis contributes to hypoxia-induced pulmonary hypertension. Am. J. Physiol. Lung Cell Mol. Physiol. *318*, 472–482. https://doi.org/10.1152/ajplung.00405.2019.

15. Qu, Z., Zhou, J., Zhou, Y., Xie, Y., Jiang, Y., Wu, J., Luo, Z., Liu, G., Yin, L., and Zhang, X.L. (2020). Mycobacterial EST12 activates a RACK1-NLRP3-gasdermin D pyroptosis-IL-1β immune pathway. Sci. Adv. *6*, eaba4733. https://doi.org/10.1126/sciadv.aba4733.

16. Koh, E.H., Yoon, J.E., Ko, M.S., Leem, J., Yun, J.Y., Hong, C.H., Cho, Y.K., Lee, S.E., Jang, J.E., Baek, J.Y., et al. (2020). Sphingomyelin synthase 1 mediates hepatocyte pyroptosis to trigger non-alcoholic steatohepatitis. Gut *70*, 1954–1964. https://doi.org/10.1136/gutjnl-2020-322509.

17. Xu, Y., Xi, J., Wang, G., Guo, Z., Sun, Q., Lu, C., Ma, L., Wu, Y., Jia, W., Zhu, S., et al. (2021). PAUPAR and PAX6 sequentially regulate human embryonic stem cell cortical differentiation. Nucleic Acids Res. *49*, 1935–1950. https://doi.org/10.1093/nar/gkab030.

18. Andric, V., Nevers, A., Hazra, D., Auxilien, S., Menant, A., Graille, M., Palancade, B., and Rougemaille, M. (2021). A scaffold lncRNA shapes the mitosis to meiosis switch. Nat. Commun. *12*, 770. https://doi.org/10.1038/s41467-021-21032-7.

19. Qin, Y., Hou, Y., Liu, S., Zhu, P., Wan, X., Zhao, M., Peng, M., Zeng, H., Li, Q., Jin, T., et al. (2021). A novel long non-coding RNA lnc030 maintains breast cancer stem cell stemness by stabilizing SQLE mRNA and increasing cholesterol synthesis. Adv. Sci. *8*, 2002232. https://doi.org/10.1002/advs.202002232.

20. Zhang, Y., Zhang, X., Cai, B., Li, Y., Jiang, Y., Fu, X., Zhao, Y., Gao, H., Yang, Y., Yang, J., et al. (2021). The long noncoding RNA lncCIRBIL disrupts the nuclear translocation of Bclaf1 alleviating cardiac ischemia-reperfusion injury. Nat. Commun. *12*, 522. https://doi.org/10.1038/s41467-020-20844-3.

21. Wan, P., Su, W., Zhang, Y., Li, Z., Deng, C., Li, J., Jiang, N., Huang, S., Long, E., and Zhuo, Y. (2020). LncRNA H19 initiates microglial pyroptosis and neuronal death in

retinal ischemia/reperfusion injury. Cell Death Differ. 27, 176–191. https://doi.org/10.1038/s41418-019-0351-4.

22. Guo, B., Wu, S., Zhu, X., Zhang, L., Deng, J., Li, F., Wang, Y., Zhang, S., Wu, R., Lu, J., and Zhou, Y. (2020). Micropeptide CIP2A-BP encoded by LINC00665 inhibits triple-negative breast cancer progression. EMBO J. 39, e102190. https://doi.org/10.15252/embj.2019102190.

23. Huang, J.Z., Chen, M., Chen, D., Gao, X.C., Zhu, S., Huang, H., Hu, M., Zhu, H., and Yan, G.R. (2017). A peptide encoded by a putative lncRNA HOXB-AS3 suppresses colon cancer growth. Mol. Cell 68, 171–184.e6. https://doi.org/10.1016/j.molcel.2017.09.015.

24. Li, Y., Zhang, J., Sun, H., Chen, Y., Li, W., Yu, X., Zhao, X., Zhang, L., Yang, J., Xin, W., et al. (2021). lnc-Rps4l-encoded peptide RPS4XL regulates RPS6 phosphorylation and inhibits the proliferation of PASMCs caused by hypoxia. Mol. Ther. J. Am. Soc. Gene Ther. 29, 1411–1424. https://doi.org/10.1016/j.ymthe.2021.01.005.

25. Liu, Y., Zhang, H., Li, Y., Yan, L., Du, W., Wang, S., Zheng, X., Zhang, M., Zhang, J., Qi, J., et al. (2020). Long noncoding RNA Rps4l mediates the proliferation of hypoxic pulmonary artery smooth muscle cells. Hypertension 76, 1124–1133. https://doi.org/10.1161/hypertensionaha.120.14644.

26. Kulkarni, P., Dasgupta, P., Hashimoto, Y., Shiina, M., Shahryari, V., Tabatabai, Z.L., Yamamura, S., Tanaka, Y., Saini, S., Dahiya, R., and Majid, S. (2021). A lncRNA TCL6-miR-155 interaction regulates the src-akt-EMT network to mediate kidney cancer progression and metastasis. Cancer Res. 81, 1500–1512. https://doi.org/10.1158/0008-5472.Can-20-0832.

27. Hu, J.J., Zhou, C., Luo, X., Luo, S.Z., Li, Z.H., Xu, Z.X., and Xu, M.Y. (2021). Linc-SCRG1 accelerates progression of hepatocellular carcinoma as a ceRNA of miR26a to derepress SKP2. J. Exp. Clin. Cancer Res. 40, 26. https://doi.org/10.1186/s13046-020-01825-2.

28. Jan, R.L., Yang, S.C., Liu, Y.C., Yang, R.C., Tsai, S.P., Huang, S.E., Yeh, J.L., and Hsu, J.H. (2020). Extracellular heat shock protein HSC70 protects against lipopolysaccharide-induced hypertrophic responses in rat cardiomyocytes. Biomed. Pharmacother. 128, 110370. https://doi.org/10.1016/j.biopha.2020.110370.

29. Sulistyowati, E., Lee, M.Y., Wu, L.C., Hsu, J.H., Dai, Z.K., Wu, B.N., Lin, M.C., and Yeh, J.L. (2018). Exogenous heat shock cognate protein 70 suppresses LPS-induced inflammation by down-regulating NF-κB through MAPK and MMP-2/-9 pathways in macrophages. Molecules 23, 2124. https://doi.org/10.3390/molecules23092124.

30. Schjoldager, K.T., Narimatsu, Y., Joshi, H.J., and Clausen, H. (2020). Global view of human protein glycosylation pathways and functions. Nat. Rev. Mol. Cell Biol. 21, 729–749. https://doi.org/10.1038/s41580-020-00294-x.

31. Chatham, J.C., Zhang, J., and Wende, A.R. (2021). Role of O-linked N-acetylglucosamine protein modification in cellular (Patho)Physiology. Physiol. Rev. 101, 427–493. https://doi.org/10.1152/physrev.00043.2019.

32. Song, X., Zhou, Z., Li, H., Xue, Y., Lu, X., Bahar, I., Kepp, O., Hung, M.C., Kroemer, G., and Wan, Y. (2020). Pharmacologic suppression of B7-H4 glycosylation restores antitumor immunity in immune-cold breast cancers. Cancer Discov. 10, 1872–1893. https://doi.org/10.1158/2159-8290.Cd-20-0402.

33. Wilson, K.D., Ameen, M., Guo, H., Abilez, O.J., Tian, L., Mumbach, M.R., Diecke, S., Qin, X., Liu, Y., Yang, H., et al. (2020). Endogenous retrovirus-derived lncRNA BANCR promotes cardiomyocyte migration in humans and non-human primates. Dev. Cell 54, 694–709.e9. https://doi.org/10.1016/j.devcel.2020.07.006.

34. Hu, Q., Ye, Y., Chan, L.C., Li, Y., Liang, K., Lin, A., Egranov, S.D., Zhang, Y., Xia, W., Gong, J., et al. (2019). Oncogenic lncRNA downregulates cancer cell antigen presentation and intrinsic tumor suppression. Nat. Immunol. 20, 835–851. https://doi.org/10.1038/s41590-019-0400-7.

35. Xing, Y., Zheng, X., Fu, Y., Qi, J., Li, M., Ma, M., Wang, S., Li, S., and Zhu, D. (2019). Long noncoding RNA-maternally expressed gene 3 contributes to hypoxic pulmonary hypertension. Mol. Ther. 27, 2166–2181. https://doi.org/10.1016/j.ymthe.2019.07.022.

36. Zehendner, C.M., Valasarajan, C., Werner, A., Boeckel, J.N., Bischoff, F.C., John, D., Weirick, T., Glaser, S.F., Rossbach, O., Jaé, N., et al. (2020). Long noncoding RNA TYKRIL plays a role in pulmonary hypertension via the p53-mediated regulation of PDGFRβ. Am. J. Respir. Crit. Care Med. 202, 1445–1457. https://doi.org/10.1164/rccm.201910-2041OC.

37. Wang, S., Cao, W., Gao, S., Nie, X., Zheng, X., Xing, Y., Chen, Y., Bao, H., and Zhu, D. (2019). TUG1 regulates pulmonary arterial smooth muscle cell proliferation in pulmonary arterial hypertension. Can. J. Cardiol. 35, 1534–1545. https://doi.org/10.1016/j.cjca.2019.07.630.

38. Matsumoto, A., and Nakayama, K.I. (2018). Hidden peptides encoded by putative noncoding RNAs. Cell Struct. Funct. 43, 75–83. https://doi.org/10.1247/csf.18005.

39. Rion, N., and Rüegg, M.A. (2017). LncRNA-encoded peptides: more than translational noise? Cell Res. 27, 604–605. https://doi.org/10.1038/cr.2017.35.

40. Nelson, B.R., Makarewich, C.A., Anderson, D.M., Winders, B.R., Troupes, C.D., Wu, F., Reese, A.L., McAnally, J.R., Chen, X., Kavalali, E.T., et al. (2016). A peptide encoded by a transcript annotated as long noncoding RNA enhances SERCA activity in muscle. Science 351, 271–275. https://doi.org/10.1126/science.aad4076.

41. Wang, J., Zhu, S., Meng, N., He, Y., Lu, R., and Yan, G.R. (2019). ncRNA-encoded peptides or proteins and cancer. Mol. Ther. 27, 1718–1725. https://doi.org/10.1016/j.ymthe.2019.09.001.

42. Meng, N., Chen, M., Chen, D., Chen, X.H., Wang, J.Z., Zhu, S., He, Y.T., Zhang, X.L., Lu, R.X., and Yan, G.R. (2020). Small protein hidden in lncRNA LOC90024 promotes "cancerous" RNA splicing and tumorigenesis. Adv. Sci. 7, 1903233. https://doi.org/10.1002/advs.201903233.

43. Liang, C., Liu, Y., Xu, H., Huang, J., Shen, Y., Chen, F., and Luo, M. (2021). Exosomes of human umbilical cord MSCs protect against hypoxia/reoxygenation-induced pyroptosis of cardiomyocytes via the miRNA-100-5p/FOXO3/NLRP3 pathway. Front. Bioeng. Biotechnol. 8, 615850. https://doi.org/10.3389/fbioe.2020.615850.

44. Jiang, Q., Geng, X., Warren, J., Eugene Paul Cosky, E., Kaura, S., Stone, C., Li, F., and Ding, Y. (2020). Hypoxia inducible factor-1α (HIF-1α) mediates NLRP3 inflammasome-dependent-pyroptotic and apoptotic cell death following ischemic stroke. Neuroscience 448, 126–139. https://doi.org/10.1016/j.neuroscience.2020.09.036.

45. Zhao, L., Oliver, E., Maratou, K., Atanur, S.S., Dubois, O.D., Cotroneo, E., Chen, C.N., Wang, L., Arce, C., Chabosseau, P.L., et al. (2015). The zinc transporter ZIP12 regulates the pulmonary vascular response to chronic hypoxia. Nature 524, 356–360. https://doi.org/10.1038/nature14620.

46. Behr, J., Nathan, S.D., Wuyts, W.A., Mogulkoc Bishop, N., Bouros, D.E., Antoniou, K., Guiot, J., Kramer, M.R., Kirchgaessler, K.U., Bengus, M., et al. (2021). Efficacy and safety of sildenafil added to pirfenidone in patients with advanced idiopathic pulmonary fibrosis and risk of pulmonary hypertension: a double-blind, randomised, placebo-controlled, phase 2b trial. Lancet Respir. Med. 9, 85–95. https://doi.org/10.1016/s2213-2600(20)30356-8.

47. Chen, B.H., Chang, Y.J., Lin, S., and Yang, W.Y. (2020). Hsc70/Stub1 promotes the removal of individual oxidatively stressed peroxisomes. Nat. Commun. 11, 5267. https://doi.org/10.1038/s41467-020-18942-3.

48. Parent, R., Qu, X., Petit, M.A., and Beretta, L. (2009). The heat shock cognate protein 70 is associated with hepatitis C virus particles and modulates virus infectivity. Hepatology 49, 1798–1809. https://doi.org/10.1002/hep.22852.

49. Niyaz, Y., Frenz, I., Petersen, G., and Gehring, U. (2003). Transcriptional stimulation by the DNA binding protein Hap46/BAG-1M involves hsp70/hsc70 molecular chaperones. Nucleic Acids Res. 31, 2209–2216. https://doi.org/10.1093/nar/gkg303.

50. Boix, C.P., Lopez-Font, I., Cuchillo-Ibañez, I., and Sáez-Valero, J. (2020). Amyloid precursor protein glycosylation is altered in the brain of patients with Alzheimer's disease. Alzheimer's Res. Ther. 12, 96. https://doi.org/10.1186/s13195-020-00664-9.

51. Losev, Y., Frenkel-Pinter, M., Abu-Hussien, M., Viswanathan, G.K., Elyashiv-Revivo, D., Geries, R., Khalaila, I., Gazit, E., and Segal, D. (2021). Differential effects of putative N-glycosylation sites in human Tau on Alzheimer's disease-related neurodegeneration. Cell. Mol. Life Sci. 78, 2231–2245. https://doi.org/10.1007/s00018-020-03643-3.

52. Kodama, H., Yoneyama, T., Tanaka, T., Noro, D., Tobisawa, Y., Yamamoto, H., Suto, S., Hatakeyama, S., Mori, K., Yoneyama, T., et al. (2021). N-glycan signature of serum immunoglobulins as a diagnostic biomarker of urothelial carcinomas. Cancer Med. 10, 1297–1313. https://doi.org/10.1002/cam4.3727.

53. Dufour, F., Rattier, T., Shirley, S., Picarda, G., Constantinescu, A.A., Morlé, A., Zakaria, A.B., Marcion, G., Causse, S., Szegezdi, E., et al. (2017). N-glycosylation of mouse TRAIL-R and human TRAIL-R1 enhances TRAIL-induced death. Cell Death Differ. 24, 500–510. https://doi.org/10.1038/cdd.2016.150.

54. Xi, H., Zhang, Y., Xu, Y., Yang, W.Y., Jiang, X., Sha, X., Cheng, X., Wang, J., Qin, X., Yu, J., et al. (2016). Caspase-1 inflammasome activation mediates homocysteine-induced pyrop-apoptosis in endothelial cells. Circ. Res. *118*, 1525–1539. https://doi.org/10.1161/circresaha.116.308501.

55. Zhang, J., Li, Y., Qi, J., Yu, X., Ren, H., Zhao, X., Xin, W., He, S., Zheng, X., Ma, C., et al. (2020). Circ-calm4 serves as an miR-337-3p sponge to regulate Myo10 (myosin 10) and promote pulmonary artery smooth muscle proliferation. Hypertension *75*, 668–679. https://doi.org/10.1161/hypertensionaha.119.13715.

56. Wu, J., Chen, S., Liu, H., Zhang, Z., Ni, Z., Chen, J., Yang, Z., Nie, Y., and Fan, D. (2018). Tunicamycin specifically aggravates ER stress and overcomes chemoresistance in multidrug-resistant gastric cancer cells by inhibiting N-glycosylation. J. Exp. Clin. Cancer Res. *37*, 272. https://doi.org/10.1186/s13046-018-0935-8.